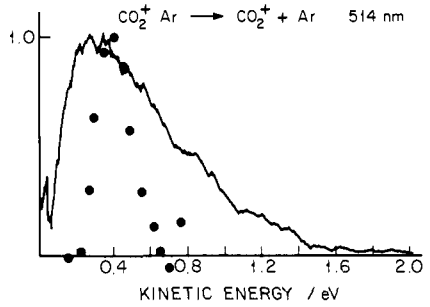

Figure 15. Plots of the kinetic energy distributions of the CO_2^+ product from both the photodissociation of CO_2^+·Ar (this work) and from the Ar^+/CO_2 charge-transfer reaction (ref 16). The points are for the charge-transfer reaction,and the line for photodissociation.

evidence to support this suggestion.

It does appear that CO_2^+/Ar products are formed by the same mechanism regardless of whether CO_2·Ar^{+*} is formed by ion–molecule reaction or photoexcitation of CO_2^+·Ar. This suggestion is supported by the data in Figure 15. In this figure the CO_2^+ kinetic energy distributions from both photoexcitation of CO_2^+·Ar and the charge-transfer reaction (eq 1) are given.[16,39] Both distributions are very similar, peaking at about 0.4 eV. It is not surprising that they differ to some extent given the very different experimental procedures used and the somewhat different energy and angular momentum distributions of the excited CO_2·Ar^{+*} ions. Since the photodissociation process must proceed via an intimate CO_2·Ar^{+*} complex, the implication is that the charge-transfer reaction also does and such long-range processes as electron jump are not important in this case.

Summary and Conclusions

(1) Photodissociation of CO_2^+·Ar results in two product ions, CO_2^+ and Ar^+. The fraction of CO_2^+ formed varies from ~5% at 458 nm to ~14% at 514 nm. This result is in qualitative agreement with the bimolecular charge-transfer reaction

$$Ar^+ + CO_2 \rightarrow CO_2^+ + Ar$$

which shows a decrease in the rate constant with increasing Ar^+ kinetic energy.[15b] The similarities of the present photodissociation study and the charge-transfer reaction are presented.

(2) The total photodissociation cross section is approximately constant at 11×10^{-18} cm^2 over the wavelength range studied.

(3) Kinetic energy release distributions for production of Ar^+ are bimodal. The 0° and 90° peak shapes indicated that Ar^+ is produced by two mechanisms, one which is fast and the other slow relative to the rotational time scale. We propose that the slow pathway is due to statistical decomposition of a bound CO_2·Ar^+ cluster ion and is a minor process while the fast pathway is the result of direct fragmentation from a repulsive surface and is the major process.

(4) The kinetic energy distributions are consistent with the fast process forming the CO_2 photofragments vibrationally excited in the ν_1 symmetric stretch. The highest level allowed by conservation of energy is formed at all photon energies. The CO_2 neutral fragment has little rotational energy, suggesting a T-shaped or linear CO_2^+·Ar complex, although a slightly nonlinear complex cannot be ruled out.

(5) The kinetic energy release distribution and 0° and 90° peak shapes for CO_2^+ show that CO_2^+ is formed via a slow mechanism with a large kinetic energy release. The kinetic energy release distribution is peaked at ~0.4 eV. These observations are consistent with electronic predissociation of a bound CO_2·Ar^+ surface to a repulsive surface leading to ground-state CO_2^+/Ar products.

Acknowledgment. We gratefully acknowledge the support of the Air Force Office of Scientific Research under Grant AFOSR-82-0035 and the National Science Foundation under Grant CHE80-20464.

Registry No. Co_2^+, 12181-61-2; Ar^+, 14791-69-6.

(39) O'Keefe, A.; Parent, D.; Bowers, M. T., unpublished data.

Structure Revision of the Antibiotic Pulvomycin

Richard J. Smith,[†] Dudley H. Williams,*[†] Jennifer C. J. Barna,[†] Ian R. McDermott,[‡] Klaus D. Haegele,[‡] Francois Piriou,[‡] Joseph Wagner,[‡] and William Higgins[‡]

Contribution from the University Chemical Laboratories, Cambridge, United Kingdom CB2 1EW, and Merrell Dow Research Institute, 67084 Strasbourg, France.
Received October 15, 1984

Abstract: The hitherto accepted structure of the antibiotic pulvomycin (also known as labilomycin) (**1**) has been shown to be incorrect. Fast atom bombardment mass spectrometry has shown pulvomycin to have a molecular weight of 838, and high field NMR experiments have allowed the structure **2** to be deduced. Pulvomycin, which inhibits prokaryotic protein biosynthesis by binding to prokaryotic elongation factor Tu, has been shown by this study to possess a triene system, two trienone systems, and an unusual 22-membered lactone ring. It also contains one sugar unit, labilose, the previously deduced stereochemistry of which has been confirmed. The relative stereochemistries of six of the eight chiral centers in the aglycone have been established by NMR studies, and the ^{13}C NMR spectrum of pulvomycin has been almost completely assigned by use of a two-dimensional heteronuclear chemical shift correlation experiment.

The antibiotic pulvomycin was first reported in 1957[1] and was subsequently "rediscovered" in 1963[2] and its structure determined.[3] The latter isolate was named labilomycin because of its extreme lability but was subsequently shown by Tishler's group[4] to be identical with pulvomycin. The comparison was based on UV and IR spectral data, pulvomycin having a very characteristic UV

[†] University of Cambridge.
[‡] Merrell Dow Research Institute.

(1) Zief, M.; Woodside, R.; Schmitz, H. *Antibiotic Chemother. (Basel, 1954—70)* **1957**, *7*, 384–386.
(2) Akita, E.; Maeda, K.; Umezawa, H. *J. Antibiot., Ser. A.* **1963**, *16*, 147–151.

0002-7863/85/1507-2849$01.50/0

Scheme I. Recycling of EF-Tu and the Sites of Action of Pulvomycin and Kirromycin

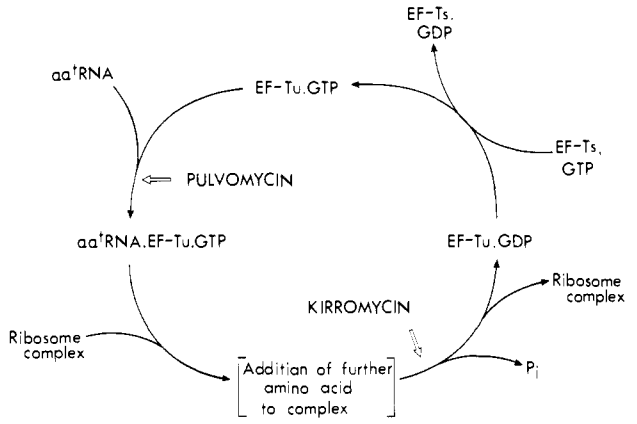

Table I. Sensitivity of *Bacillus subtilis* to Pulvomycin[a]

amt of pulvomycin,[b] pmol		diam of inhibition zone, mm	
bioassay 1	bioassay 2	bioassay 1	bioassay 2
35	33	12	12
70	66	14	14
140	132	16	16
211	219	18	16

[a] Agar diffusion test: diameter of filter disks 9 mm: medium N-Broth with 15 g/L agar overlaid with *B. subtilis* freshly grown overnight in "top agar". [b] Pulvomycin applied in 50 μL of MeOH; concentration determined via λ_{max} 320 nm ($E^{1\%}_{1cm}$ = 890). Bioassay 1 carried out on purified pulvomycin; bioassay 2 carried out after a 3-h NMR experiment performed at 20 °C in $CDCl_3$ solution.

spectrum. Although the proposed structure[3] of pulvomycin (**1**) has been accepted for 20 years, it was cast into doubt by discrepancies between structure **1** and the published NMR data.[4]

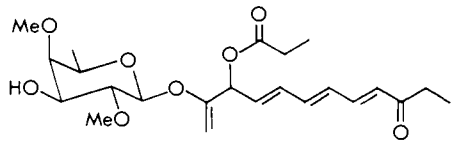

1

Interest in the correct structure of pulvomycin was renewed when it was shown that it had a unique mode of action:[5] the prevention of the formation of a ternary complex between prokaryotic elongation factor Tu (EF-Tu), guanosine 5′-triphosphate (GTP), and aminoacyl-tRNA (α,α-tRNA), which is an essential step in the biosynthesis of protein. This site of action is shown in Scheme I together with that of kirromycin, an antibiotic with the same target protein but a different mechanism of action.[6]

That elongation factor Tu (EF-Tu) is an important target may be argued on teleological grounds. It is coded for by two genes in *E. coli*[7] and in many other bacteria so far studied.[8] In addition, the conservation of genetic sequence[8] would suggest that an inhibitor of EF-Tu would have a broad spectrum of action. Although pulvomycin has a poor activity against gram-negative organisms,[9]

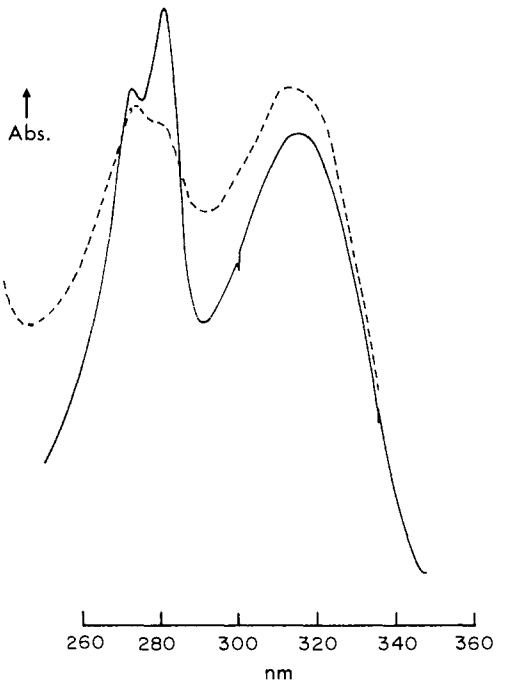

Figure 1. UV spectra of pulvomycin (solid line) and decomposition product of pulvomycin (dashed line) after separation by HPLC.

it seemed a plausible starting point for modification studies.

The joint application of fast atom bombardment mass spectrometry (FABMS) and high-field NMR spectroscopy presented in this report shows that the correct structure of pulvomycin (**2**) is considerably more complicated than that originally proposed (**1**).

Results

Extraction and Bioactivity. Pulvomycin was extracted from the crude mycelium of *Streptoverticillium netropsis* by using CH_2Cl_2/MeOH (3:1, v/v) protected from light and at 4 °C because of the known light and heat sensitivity of pulvomycin.

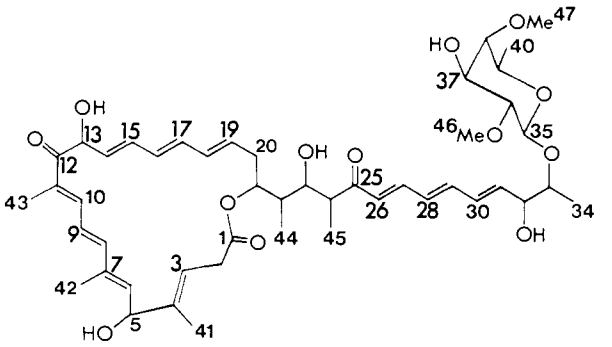

2

Several other solvent systems were tried, but although they gave more thorough extraction, other metabolites coextracted in these systems made subsequent chromatography difficult.

Since pulvomycin is both thermo- and photolabile and extended NMR experiments at room temperature were used in the structure determination, it was important to show that pulvomycin was still bioactive after such experiments. Table I shows the results of one such experiment; it is clear that the bioactivity of the pulvomycin is the same, within experimental error, before and after the 3-h experiment. This is an important point since bioinactive material, which can be separated from pulvomycin by HPLC, has similar UV spectral properties (Figure 1) to pulvomycin. In particular, the extinction coefficient ($E^{1\%}_{1cm}$) at 320 nm of this bioinactive material is almost identical with that of pulvomycin, and since this quantity is often used to calculate concentrations of active material, overestimates of pulvomycin concentrations can be made. For example, data presented by Wolf et al.[5] showed that pulvo-

(3) Akita, E.; Maeda, K.; Umezawa, H. *J. Antibiot. Ser. A* **1964**, *17*, 200–215.
(4) Schwartz, J. L.; Tishler, M.; Arison, B. H.; Shafer, H.; Omura, S. *J. Antibiot.* **1976**, *29*, 236–241.
(5) Wolf, H.; Assmann, D.; Fischer, E. *Proc. Natl. Acad. Sci. U.S.A.* **1978**, *75*, 5324–5328.
(6) Pingoud, A.; Urbanke, C.; Wolf, H.; Maas, G. *Eur. J. Biochem.* **1978**, *86*, 153–157.
(7) Jaskunas, S. R.; Lindahl, L.; Nomura, M.; Burgess, R. R. *Nature (London)* **1975**, *257*, 458–462.
(8) Filer, D.; Furano, A. V. *J. Biol. Chem.* **1980**, *255*, 728–734.
(9) Umezawa, H.; Akita, E. Japanese Patent, 11 367, 1963.

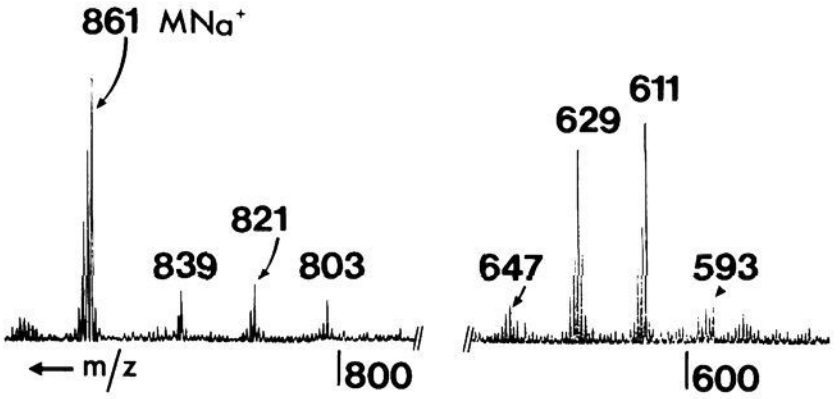

Figure 2. Positive ion FAB mass spectrum of pulvomycin.

Scheme II. Major Fragmentations of Pulvomycin in Mass Spectrometry

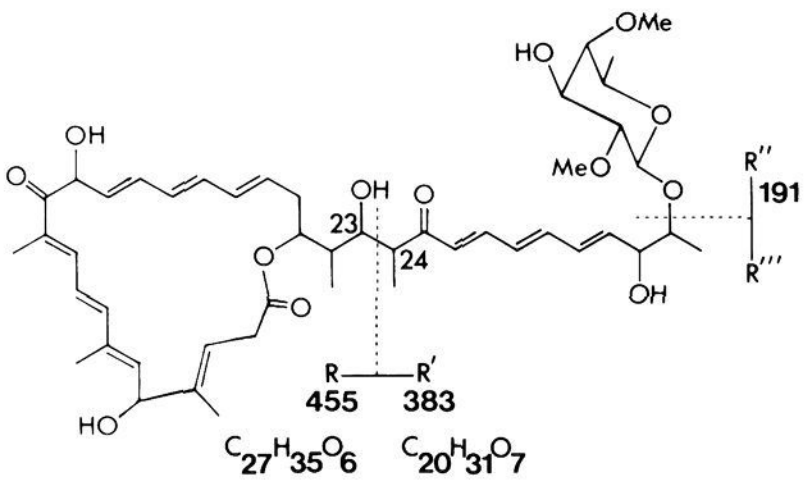

mycin blocked in vivo poly-U programmed poly(Phe) protein synthesis with an EC_{50} of $1-2 \times 10^{-6}$ M. We obtained similar results initially, but after removal of bioinactive materials absorbing at 320 nm by HPLC, we now report an EC_{50} of $1-2 \times 10^{-7}$ M. This latter figure also includes a correction for the new molecular weight of pulvomycin.

Mass Spectrometric Studies. Initial studies using electron impact mass spectrometry (EIMS), and chemical ionization mass spectrometry (CIMS) using methane as reagent gas, failed to give molecular weight information on pulvomycin. However, both EIMS of *O*-trimethylsilyl-d_9 (TMS-d_9) pulvomycin and CIMS of underivatized pulvomycin gave fragment ions which could be rationalized, after the covalent structure of pulvomycin had been determined by later NMR studies, as resulting from C-23, C-24 bond cleavage with hydrogen transfer (see Scheme II). Thus, CIMS yielded fragment ions at m/z 455 (R^+) and 385 ($R'H_2^+$). Two other fragment ions at m/z 437 and 419 could be rationalized as being due to the sequential loss of two molecules of H_2O from R^+, and a further (major) fragment ion at m/z 393 could be interpreted as $(R - CO_2 - H_2O)^+$. Labilose was identified by fragmentation around the β-glycosidic oxygen, yielding ions at m/z 175 and 193 ($R''H_2^+$). Both of these ions were appropriately displaced in the spectra of TMS and TMS-d_9 derivatives.

Subjecting a TMS-d_9 derivative of pulvomycin to EIMS produced ions at m/z 697 and 616, corresponding to $[(TMS\text{-}d_9)_3(R - H)]^{+\cdot}$ and $[(TMS\text{-}d_9)_2(R - H)]^{+\cdot}$, respectively. This result confirms the presence of three hydroxy groups in the R moiety, as required by structure **2**.

Fast atom bombardment mass spectrometry[10] (FABMS) of pulvomycin produced not only fragment ions but also intact pseudomolecular ions, thus enabling the first molecular weight determination of this antibiotic to be made. Positive and negative ion FAB mass spectra are shown in Figures 2 and 3, respectively. In the positive ion spectrum, the MNa^+ occurs at m/z 861 with a less abundant MH^+ at m/z 839. Sequential losses of nH_2O molecules (n = 1, 2, 3) from the MH^+ give rise to ions at m/z 821, 803, and 785. A metastable ion at m/z 803.5 (not apparent in Figure 2) supports the direct loss of H_2O from MH^+ to give m/z 821: this latter ion is therefore not due to an impurity. Ions at m/z 647, 629, 611, and 593 correspond to $R'''^+ - nH_2O$ where

(10) Barber, M.; Bordoli, R. S.; Sedgwick, R. D.; Tyler, A. N. *J. Chem. Soc., Chem. Commun.* **1981**, 325–327.

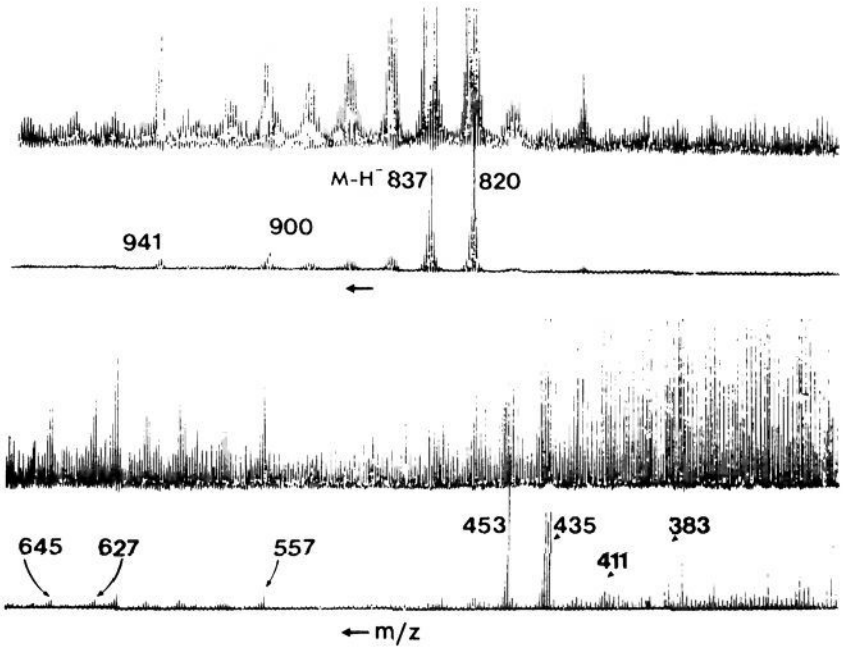

Figure 3. Negative ion FAB mass spectrum of pulvomycin.

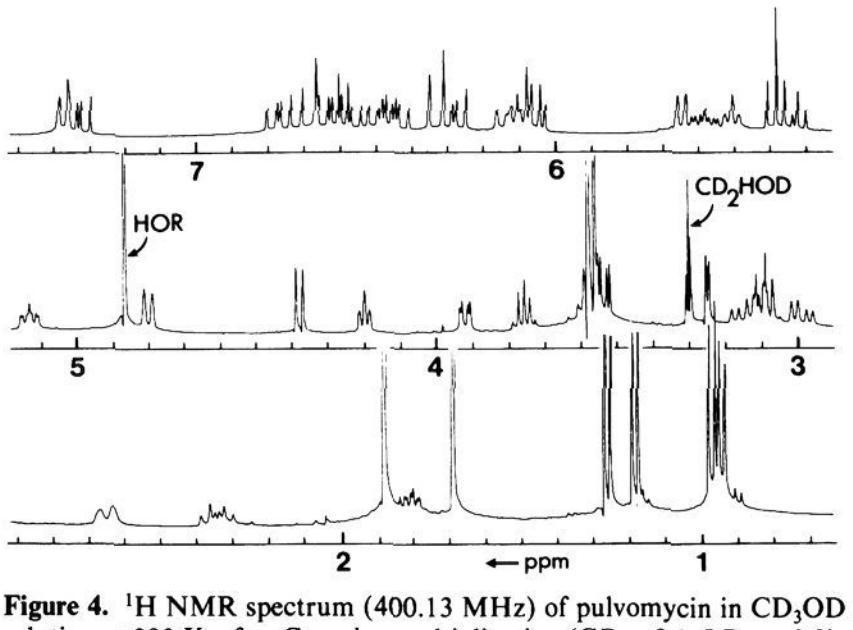

Figure 4. ^1H NMR spectrum (400.13 MHz) of pulvomycin in CD_3OD solution at 293 K, after Gaussian multiplication (GB = 0.3, LB = −0.8).

n = 0, 1, 2, and 3, respectively, and R''' has the structure shown in Scheme II. Note that there is apparently no C-23, C-24 bond cleavage under FAB conditions which results in positively charged fragment ions.

In the negative ion FAB mass spectrum, the $(M - H)^-$ appears at m/z 837. An $[(M - H)^- + 63]$ adduct ion appears at m/z 900; although such adduct peaks have been observed in our laboratory on several occasions with various compounds in the negative ion mode, we are unsure of their origins. The appearance of several ions at *even* m/z values indicates the formation of relatively stable radical anions under FAB conditions. The species at m/z 820 is such a radical anion and probably results from the loss of H_2O from an $M^{-\cdot}$ at m/z 838 which is presumably too unstable to be detected. A metastable ion at m/z 802.5 supports this deduction. Although radical anions are unusual in FAB spectra, the extended enone chromophores of pulvomycin (**2**) will promote the formation of such species. The fragmentation of $(M - H_2O)^{-\cdot}$, or possibly of M^-, then accounts for the ion observed at m/z 436 $[(R - H - H_2O)^{-\cdot}]$. Even-electron anions associated with cleavage of the same C–C bond occur at m/z 435 and 437. The ions at m/z 453 and 383 correspond to $(R-2H)^-$ and R'^-, respectively, and probably result from cleavage of the $(M - H)^-$ ion. The ion at m/z 411 could correspond to $(R' + CO)^-$ and result from the cleavage of the C-22, C-23 bond. Ions at m/z 645 and 627 correspond to $(R'''-2H)^-$ and $(R'''-H_2O-2H)^-$, respectively.

The species at m/z 941 appears to be a matrix adduct to the ion at m/z 820; a species at m/z 1004 (not shown) appears to be a (matrix + 63) adduct to the same ion. Similarly, the species at m/z 557 is a matrix adduct to m/z 436 or possibly m/z 435.

Mass spectrometry thus shows pulvomycin to have a molecular weight of 838: the fragment ions produced under a variety of conditions can be rationalized in terms of structure **2**, with the major fragmentations occurring at expected sites.

NMR Studies. A 400-MHz ^1H NMR spectrum of pulvomycin in CD_3OD solution at 293 K is shown in Figure 4. Obvious features of the spectrum are the two downfield signals, one a doublet and the other a doublet of doublets, between δ 7.2 and 7.4, which are characteristic of protons on the β carbons of α,β-unsaturated carbonyl groups. The anomeric proton is also clearly assigned as δ 4.38. Decoupling difference experiments on pulvomycin (see ref 11 for a recent review of the use of difference spectroscopy in nuclear magnetic double-resonance experiments), using first CD_3OD as the solvent at 293 K and then $(CD_3)_2SO$ at the same temperature, enabled the partial structures **3**–**7** to be deduced. In **3**–**7**, the δ values are taken from $(CD_3)_2SO$

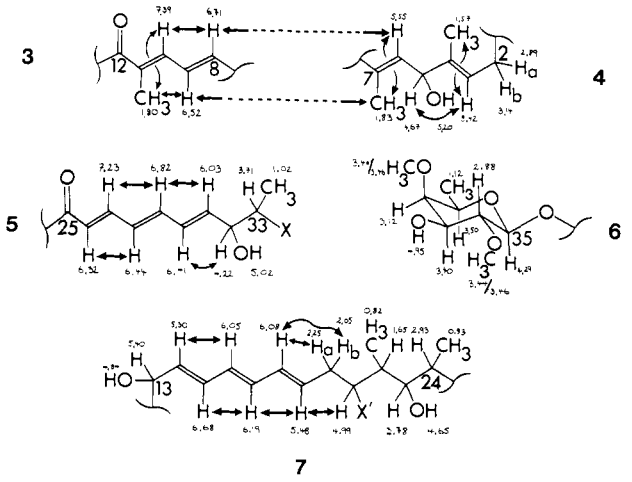

7

solution, curved arrows show allylic couplings observed in $(CD_3)_2SO$ and/or CD_3OD solutions, and straight arrows show some of the nuclear Overhauser effects (nOes) observed in $(CD_3)_2SO$ solution. The structure and stereochemistry of the labilose moiety (**6**) had already been established by previous workers:[3] the present work confirms the stereochemistry ascribed. The chemical shifts (in CD_3OD and $(CD_3)_2SO$ solutions) of all 66 protons and their coupling constants (in CD_3OD) are presented in Table II. The greater line widths in $(CD_3)_2SO$ solution, together with less chemical shift dispersion of the signals with respect to CD_3OD solution, made accurate measurement of coupling constants in $(CD_3)_2SO$ difficult. The coupling constants measured in this solvent were, however, similar to their counterparts found in CD_3OD solution.

The magnitudes of the ^1H–^1H coupling constants across the double bonds (14.5–15.5 Hz) establish[12] the majority of the double bond configurations as *E*. For the trisubstituted double bonds, namely those between C-3 and C-4, C-6 and C-7, and between C-10 and C-11, there is no coupling constant information and the geometries must be established by using nuclear Overhauser effects[13–15] (nOes). In both CD_3OD and $(CD_3)_2SO$ solutions, the nOes observed between protons in pulvomycin were negative at 293 K: they were more negative in the more viscous $(CD_3)_2SO$[16,17] so this solvent was used for the nOe difference experiments. Table III gives details of the nOes observed in $(CD_3)_2SO$ solution. In separate irradiations of H-10, δ 7.39, and of H-6, δ 5.55 (these proton chemical shift values and all those given later in the text refer to $(CD_3)_2SO$ solution), negative enhancements of H-8, δ 6.71, could be obseved by using nOe difference spectroscopy. The reverse experiment, that is, irradiation of H-8, lead to negative enhancements of H-10 and H-6. Similarly, irradiation of H-9, δ 6.52, leads to negative enhancements of H-42, δ 1.83, and H-43, δ 1.80. These results establish not only the connection between fragments **3** and **4** but also the *E* configuration of the double bonds between C-6 and C-7 and between C-10 and C-11. The configuration of the isolated double bond between C-3 and C-4 is more difficult to establish: it has no conformational requirements imposed on it by conjugation. Proof that is has the *E* configuration by observation of selective nOes to neighboring protons depends on there being very distinct differences in interproton distances between the *E* and *Z* forms: an obvious interproton distance which must change is that between H-3 and H-41. It is noted that there is *no* change in the intensity of the signal due to H-3, δ 5.42, when H-41, δ 1.57, is irradiated nor does the intensity of H-41 change when H-3 is irradiated. The configuration of the C-3, C-4 double bond is therefore tentatively assigned as *E*, since an nOe would be expected if the C-41 methyl group and H-3 were cis to each other.

Table II. ^1H NMR (400 MHz) Signals of Pulvomycin, Their Assignment and Coupling Constants

δ (CD_3OD) ±0.01 ppm	coupling constants ±0.03, Hz (CD_3OD)	assignment	δ [$(CD_3)_2SO$] ±0.01 ppm
7.37 d	10.5, *a*	H-10	7.39
7.33 dd	15.5, 11.0	H-27	7.23
6.77 dd	14.5, 11.0	H-29	6.82
6.69 d	15.0	H-8	6.71
6.63 dd	14.5, 10.5	H-15	6.68
6.57 dd	15.0, 10.5	H-9	6.52
6.49 dd	15.0, 11.0, *a*	H-30	6.41
6.44 dd	14.5, 11.0	H-28	6.44
6.34 d	15.5	H-26	6.32
6.28 dd	15.0, 10.5	H-17	6.19
6.13 dd	15.0, 10.5, *a*	H-18	6.08
6.08 dd	15.0, 10.5	H-16	6.05
6.06 dd	15.0, 5.5	H-31	6.03
5.65 d	9.0, *a*	H-6	5.55
5.58 ddd	15.0, 10.0, 4.0	H-19	5.48
5.51 br t	8.0, 7.0, *a*	H-3	5.42
5.40 d	10.0	H-13	5.40
5.33 dd	14.5, 10.0	H-14	5.30
	4.0[b]	OH-5	5.20
		OH-32	5.02
5.14 ddd	10.0, 7.5, 2.5	H-21	4.99
		OH-37	4.95
	5.5[b]	OH-13	4.84
4.80 d	9.0, *a*	H-5	4.67
		OH-23	4.65
4.38 d	7.5	H-35	4.29
4.20 br t	5.5, 5.5, *a*	H-32	4.22
3.92 dd	9.5, 2.5	H-23	3.78
3.76 dq	6.5, 5.5	H-33	3.71
3.60 m	6.0, <1	H-39	3.50
3.58 s		H-46 or 47	3.46
3.57 s		H-47 or 46	3.44
3.54 dd	10.0, 3.0	H-37	3.40
3.25 d	3.0, <1	H-38	3.12
3.15 dd	16.5, 8.0	H-26	3.14
3.10 dd	10.0, 7.5	H-36	2.88
3.08 m	9.5, 7.0	H-24	2.93
2.99 dd	16.5, 7.0	H-2a	2.89
2.65 br d	15.5, 4.0, 2.5, *a*	H-20b	2.66
2.34 ddd	15.5, 10.0, 10.0	H-20a	2.25
1.88 s	*a*	H-42[c]	1.83
1.88 s	*a*	H-43[c]	1.80
1.81 m	7.5, 7.0, 2.5	H-22	1.65
1.68 s	*a*	H-41	1.57
1.26 d	6.0	H-40	1.12
1.18 d	6.5	H-34	1.02
0.96 d	7.0	H-45	0.83
0.93	7.0	H-44	0.82

[a] Small, unresolved allylic coupling present. [b] These coupling constants measured from data collected in $(CD_3)_2SO$ experiments. [c] H-42, H-43 are coincident in CD_3OD solution at δ 1.88; they are separate in $(CD_3)_2SO$ solution with H-42 at δ 1.83.

(11) Sanders, J. K. M.; Mersh, J. D. *Prog. Nucl. Magn. Reson. Spectrosc.* **1983**, *15*, 353–400.
(12) Williams, D. H.; Fleming, I. "Spectroscopic Methods in Organic Chemistry", 3rd ed.; McGraw-Hill: London, 1980; pp 100–101.
(13) Noggle, J. H.; Schirmer, R. E. "The Nuclear Overhauser Effect"; Academic Press: New York, 1971.
(14) Balaram, P.; Bothner-By, A. A.; Dadok, J. *J. Am. Chem. Soc.* **1972**, *94*, 4015–4017.
(15) Glickson, J. D.; Gordon, S. L.; Pitner, T. P.; Agresti, D. G.; Walter, R. *Biochemistry* **1976**, *15*, 5721–5729.
(16) Szeverenyi, N. M.; Bothner-By, A. A.; Bittner, R. *J. Phys. Chem.* **1980**, *84*, 2880–2883.
(17) Williamson, M. P.; Williams, D. H. *J. Chem. Soc., Chem. Commun.* **1981**, 165–166.

Table III. Nuclear Overhauser Enhancement Observed in Pulvomycin[a]

proton irrad	nOes observed	proton irrad	nOes observed
H-2a	H-26 (1), H-3 (s), H-41 (vs)	H-22	H-21 (s),[b] H-23 (m), H-44 (m), H-45 (m)
H-2b	H-2a (1), H-3 (s)		H-24 (s), H-20b (s), H-20a (s)
H-3	H-2a (s), H-2b (s)	H-44[c]	H-21 (m), H-23 (m), H-24 (1), H-22 (1), H-23o (s)
H-5	H-42 (1), H-41 (vs)	H-23	H-23o (1), H-20b (1), H-20a (1), H-26 (m), H-22 (m), H-24 (m)[b]
H-42	H-9 (1), H-5 (1)	H-24	H-27 (1), H-26 (1), H-44 (m), H-45 (m)
H-8	H-10 (1), H-6 (1)		H-23 (s)
H-9	H-42 (1), H-43 (1)	H-45[c]	H-24 (1), H-22 (1), H-23 (m), H-26 (m)[b]
H-10	H-8 (1), H-15 (1), H-13 (1)	H-26	H-24 (m), H-45 (s), H-28 (1)
H-43	H-9 (1)	H-27	H-29 (1), H-24 (1)
H-13	H-10 (1), H-15 (1)	H-28	H-26 (1)
H-14	H-16 (m)	H-29	H-27 (1), H-31 (1)
H-15	H-10 (1), H-13 (m), H-17 (m)	H-30	H-32 (m)
H-16	H-14 (m)	H-31	H-29 (1), H-32 (m), H-33 (s)
H-17	H-15 (m), H-19 (m)	H-32	H-30 (1), H-31 (1), H-33 (m), H-32o (m)
H-18	H-20a (s)	H-33	H-35 (1), H-32 (1), H-31 (m)
H-19	H-17 (m), H-21 (m), H-20b (s)	H-34	H-33 (1), H-32 (m), H-31 (s)
H-20a	H-20b (vl), H-18 (m), H-21 (m)[b]	H-35	H-33 (m), H-39 (m), H-37 (m), H-38 (s)
	H-23 (1), H-22 (m)	H-36	
H-20b	H-20a (vl), H-23 (1), H-18 (m)[b]	H-37	H-35 (m), H-38 (s)
	H-19 (m), H-21 (m), H-22 (m)	H-38	H-37 (m), H-39 (m), H-35 (s)
H-21	H-19 (m), H-20b (s), H-22 (s)	H-39	H-38 (m), H-35 (s)
	H-23 (s)	H-40	H-39 (s), H-38 (s)

[a] These nOes were recorded after an irradiation time of 0.5 s, using a 40-dB attenuation of the 0.2-W level of decoupler power. Under these conditions, the nOes had reached ~50% of their maximum values in most cases. The sizes of the nOes in the table are indicated qualitatively as very small (vs); small, <5% (s); medium, 5–10% (m); large, >10%, (l); and very large (vl). [b] Shown to be indirect by studies of the rate of buildup of this nOe. It follows that spin diffusion had become significant at 0.5 s. [c] Irradiated using 60-dB attenuation of the 0.2-W level of decoupler power in a solution of C_6D_6 and $(CD_3)_2SO$, 7:25 v/v.

Support for this assignment is given by the observation that when H-2a, δ 2.89, is irradiated, there is a very slight negative enhancement (−0.6% under the conditions given in the footnote to Table III) of the signal due to H-41. The converse enhancement also occurs. If the C-3, C-4 double bond possessed *Z* geometry, it would be expected that H-3 would interpose between H-2a and H-41, preventing any direct nOe between them. The observation of this nOe, although it is small in both directions because of the efficient internal relaxation of both the methyl and the methylene groups, confirms the assignment of the C-3, C-4 double bond as *E*. Additionally, ^{13}C-41 has a chemical shift consistent with it being subject to the steric crowding of an *E* double bond (the γ effect[18]). The ^{13}C NMR spectrum of pulvomycin in CD_3OD solution was assigned almost completely on the basis of chemical shift and a two-dimensional ^{1}H–^{13}C chemical shift correlation experiment.[19-21] This experiment correlates the chemical shift of a proton-bearing ^{13}C with the chemical shift(s) of the proton(s) it bears, and it enabled the assignment of ^{13}C signals by reference to the previously assigned ^{1}H NMR spectrum. The ^{13}C data are presented in Table IV. Thus, ^{13}C signals at δ 12.7 and 11.9 could be assigned to C-42 and C-43 since they correlate with a proton chemical shift of δ 1.88 (CD_3OD data), and the signal at δ 14.8 could be assigned to two carbons, one of which is C-41, which correlates with a proton chemical shift of δ 1.68 (CD_3OD data). The ^{13}C chemical shifts of all three vinyl methyl groups indicate[22,23] that they are sterically crowded, as they would be if positioned on *E* double bonds. Other contributions to the steric crowding of these groups cannot be ruled out, and there is no *Z* trisubstituted double bond in pulvomycin to act as an internal reference, so that sole reliance on vinyl methyl chemical shifts to predict double bond geometry is not warranted in this case. However, the chemical shift data are consistent with an *E* geometry of the C-3, C-4 double bond, as shown by the nOe information presented above.

Table IV. ^{13}C NMR (100 MHz) Data for Pulvomycin

δ (CD_3OD)[a] ±1 ppm and multiplic	assign (C no.)	δ (CD_3OD)[a] ±1 ppm and multiplic	assign (C no.)
205.9, s (205.0)[b]	C-12 or 25	82.9, d	C-36
200.5, s (199.6)	C-25 or 12	80.6, d	C-33
173.7, s (172.9)	C-1	77.3, d	C-21
148.1, d	C-8	76.7, d	C-13
146.4, d	C-10	75.6, d	C-32
144.8, d	C-27	75.4, d	C-37
143.1, d	C-29	73.7, d	C-23
141.6, s (141.1)	C-9 or 7 or 4	72.2, d	C-5
140.5, d	C-6	71.7, d	C-39
139.0, d	C-31	62.7, d (63.1)	C-47 or 46[c]
137.8, (d)	C-15	61.4, d (61.8)	C-46 or 47[d]
135.9, d	C-17	48.8, d (47.5)	C-24
135.6, s (134.8)	C-7 or 9 or 4	40.1, d (40.1)	C-22
133.5, d	C-18 and C-19	36.9, dd (36.9)	C-20
132.3, d	C-30	34.3, dd (33.9)	C-2
132.2, d	C-14	17.6, q (18.8)	C-34
131.7, d	C-28	16.9, q (17.4)	C-40
130.9, s (130.8)	C-4 or 7 or 9	14.8, m (15.4)	C-44 and C-41
130.7, d	C-16	12.7, q (13.0)	C-42 or 43
130.3, d	C-26	11.9, q (12.4)	C-43 or 42
124.0, d (123.2)	C-9	9.3, q (9.9)	C-45
118.0, d (117.6)	C-3		
104.9, d (104.9)	C-35		
83.8, d	C-38		

[a] δ values related to the TMS scale by the relation δ(TMS) = δ (CD_3OD) + 49.05. [b] Values in parentheses are δ values in $CDCl_3$. [c] This signal correlates with the signal at δ 3.57 in the proton spectrum. [d] This signal correlates with the signal at δ 3.59 in the proton spectrum.

The other nOes shown in structures **5** and **7**, namely those from H-17 to H-15 and H-19, from H-16 to H-14, from H-29 to H-27 and H-31, and all their converses, confirm the *E* configuration for the remainder of the double bonds in pulvomycin and demonstrate that these regions are extended. Some of the nOes "expected" in structures **5**, **6**, and **7** could not be observed because of the small chemical shift differences between the observed and irradiated nuclei. Examples of such expected, but not observable, nOes are those between H-16 and H-18 ($\Delta\delta$ = 13 Hz), H-28 and H-30 ($\Delta\delta$ = 13 Hz), and H-37 and H-39 ($\Delta\delta$ = 26 Hz). However, an nOe between H-26 and H-28 ($\Delta\delta$ = 48 Hz) could be identified by using very low-power irradiations.

The number of hydroxy protons in pulvomycin was established by a saturation transfer difference experiment[11] performed in $(CD_3)_2SO$ under the same conditions as for the nOe difference experiments. The difference spectrum is shown in Figure 5, together with part of a normal 400-MHz ^{1}H spectrum in $(CD_3)_2SO$ solution. The H_2O signal, which was saturated in the experimental data set, appears as a negative peak, as do the pulvomycin hydroxy protons which have become saturated, or

(18) Grant, D. M.; Paul, E. G. *J. Am. Chem. Soc.* **1964**, *86*, 2984–2990.
(19) Bodenhausen, G.; Freeman, R. *J. Magn. Reson.* **1977**, *28*, 471–476.
(20) Freeman, R.; Morris, G. A. *J. Chem. Soc., Chem. Commun.* **1978**, 684–686.
(21) Bax, A.; Morris, G. A. *J. Magn. Reson.* **1981**, *42*, 501–505.
(22) Carey, L.; Clough, J. M.; Pattenden, G. *J. Chem. Soc., Perkin Trans. 1* **1983**, 3005–3009 and references therein.
(23) (a) Rowan, R., III; Sykes, B. D. *J. Am. Chem. Soc.* **1974**, *96*, 7000–7008. (b) Becker, R. S.; Berger, S.; Dalling, D. K.; Grant, D. M.; Pugmire, R. J. *J. Am. Chem. Soc.* **1974**, *96*, 7008–7014.

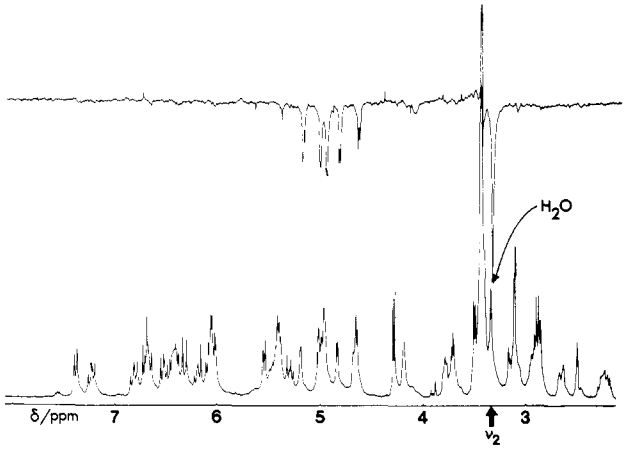

Figure 5.

partially saturated, by chemical exchange with the H_2O in the solvent. The five hydroxy protons thus identified in the NMR spectrum could then be located within the partial structures **3–7** by decoupling difference spectroscopy.

The connectivity of the partial structures **3–7** was then established by further nOe difference experiments, the relevant results of which are summarized in structure **8**. Thus, H-10 is found

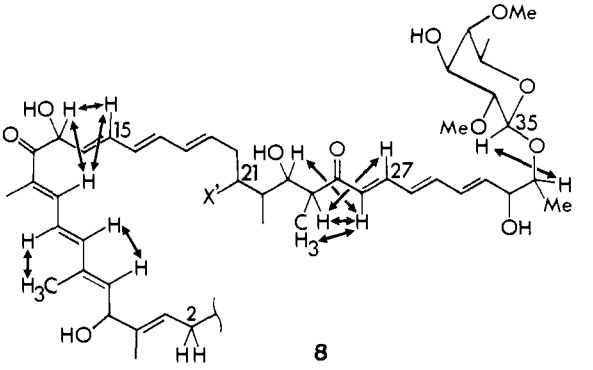

8

to be close in space to H-13 and H-15, H-23 and H-24 are close to H-26 and H-27, and H-35 is close to H-33. The proximity of H-6 to H-8 and of H-42 to H-9 has been mentioned above. This then completes the covalent structure of pulvomycin except for one linkage, that bridging C-21 and C-2. The nature of this linkage was revealed by FABMS and further consideration of the ^{13}C NMR spectrum.

The carbonyl carbons C-12 and C-25 are seen from Table IV to have chemical shifts of δ 205.9 and 200.5 (CD_3OD data): a third peak in the carbonyl region is evident at δ 173.7 and corresponds to the carbonyl carbon of an ester or lactone moiety. The molecular weight of pulvomycin, as determined by FABMS, is 838. Structure **8** has a mass of 794, that is, 44 less than the known molecular weight. Taking this information in conjunction with the ^{13}C NMR data, it is obvious that the 44 daltons is made up by a $-CO_2-$ unit, which bridges the gap between C-21 and C-2 to give structure **2**.

With three carbonyl groups in pulvomycin, it could be argued that C-12 or C-25 is the lactone/ester carbonyl carbon and not C-1. However, a lactone carbonyl at C-12 would require an α,β-unsaturated aldehyde (at C-13) to be trapped as its hydrate by lactonization: the possibility that C-12 is a lactone carbonyl is thus remote. That C-25 is unlikely to be the lactone carbonyl can be argued on the basis of proton and carbon chemical shifts. The chemical shifts of H-21 (δ 4.99) and H-24 (δ 2.93) agree with structure **2**: these shifts would fit far less well a structure in which C-25 became a lactone carbonyl carbon and C-1 a ketone. A similar argument can be based on the ^{13}C chemical shifts of C-21 and C-24, which were found, from the heteronuclear chemical shift correlation data, to be δ 77.3 and 48.8, respectively. Thus the covalent structure of pulvomycin is as shown in structure **2**.

Conformation and Relative Stereochemistry Studies. The unusual lactone ring in pulvomycin is found by model building (CPK models) to be relatively rigid although the ring can be closed without significant strain. It would thus be expected that much stereochemical and conformational data could be deduced from nOe and $^1H-^1H$ coupling constant data. In addition, the coupling constants between H-22 and H-23 (2.4 Hz) and H-23 and H-24 (9.5 Hz) suggest that there is restriction on chain mobility in this region too so that, in principle, the relative stereochemistries of C-22 to C-24 should be accessible by NMR methods. However, on the same basis, the relative stereochemistries at C-32 and C-33 would be expected to remain elusive in this nondestructive probing.

A space-filling model shows the lactone ring to be roughly triangular when viewed from above: C-12 and C-13 form one apex, C-5 forms a second, and C-20 and C-21 form the third (see **2**). The coupling constant between H-13 and H-14 is 10.0 Hz, indicating an approximately trans relationship between the two protons.[12] The observation of an nOe to H-15, δ 6.82, on irradiation of H-13 is in agreement with this. The same irradiation of H-13 also produces an nOe to H-10: irradiation of H-10 produces nOes to both H-13 and H-15. These three protons are therefore close in space—as might be expected if they are at an apex of the ring. The H-5/H-6 coupling constant is 9.0 Hz; an nOe to H-42 can be observed on irradiating H-5 (and to H-5 when H-42 is irradiated)—H-5 thus appears to be approximately trans to H-6. H-5 is also allylically coupled to H-3, suggesting that H-5 is approximately in the plane (±30°) of the π bond between C-3 and C-4.[24]

The information concerning H-20a,b and H-21 is summarized in structure **9**. The H-20a proton is thus trans to both H-19 and H-21, and H-20b is approximately in the plane of the π bond between C-18 and C-19. If then the absolute stereochemistry

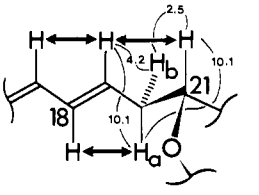

9

at C-21 is *arbitrarily* defined as *R* (as shown in **9**), the stereochemistries at C-13 and C-5 follow automatically from ring closure and the coupling constant and nOe data presented above, in Table II and in structures **4**, **5**, and **6**. Thus, the configuration at C-13 is *R* and that at C-5 is *S*, relative to the defined *R* configuration at C-21.

The relative configurations at C-22, C-23, and C-24 could be established from coupling constant data and further nOe experiments. The protons H-44 and H-45 of the two methyl groups attached to C-22 and C-24 have very similar chemical shifts in $(CD_3)_2SO$ solution (the centers of the doublets are separated by approximately 5 Hz) so that specific irradiation of either H-44 nd H-45 was not possible in this solvent. Addition of aliquots of benzene to the $(CD_3)_2SO$ solution would be expected to cause differential shielding/deshielding of protons depending on the proximity of those protons to electron-deficient or electron-rich centers in pulvomycin,[25] and it was hoped that the H-44, H-45 chemical shift separation could be increased in this way. Addition of aliquots of C_6D_6 to give a final solvent composition of $C_6D_6/(CD_3)_2SO$ = 7:25 v/v was found, on specific decoupling of each methyl doublet, to cause deshielding of H-44 relative to H-45. At this final composition, the doublet centers were separated by approximately 11.5 Hz, and not only could enhancements of either methyl signal on irradiation of other protons be observed, but also very low-power irradiations of each methyl in turn could be achieved with high selectivity. By varying the irradiation time

(24) Collins, D. J.; Hobbs, J. J.; Sternhell, S. *Aust. J. Chem.* **1963**, *16*, 1030–1041.
(25) Wilson, R. G.; Rivett, D. E. A.; Williams, D. H. *Chem. Ind.* (*London*) **1969**, 109–110.

Table V. $t_{1/2}$ Data for Interproton nOes around the C21–C22 Junction[a]

proton irrad	$t_{1/2}$ values observed (±0.1), s							
	H-8	H-20a	H-20b	H-22	H-23	H-24	H-26	H-23o
H-20a	0.6		0.25	*b*	0.45			
H-20b		0.25		*b*	0.35			
H-22		0.25	0.35		0.35	0.8		
H-23		0.35	0.25	0.5			0.75	0.55

[a] Decoupler power was sett to 40-dB attenuation of the 0.2-W level, and all experiments were carried out at approximately 293 K. Values of $t_{1/2}$s for nOes to H-44, H-45, and H-21 have been omitted from this table since overlapping signals made accurate measurements of the enhancements impossible. [b] Data not good enough to warrant calculation of $t_{1/2}$. Blanks mean no direct nOe observed to this proton in this experiment.

of each methyl group, the rates of buildup of nOes to various protons could be studied. Qualitatively, the faster an enhancement of a proton signal grows, the closer in space is that observed proton to the irradiated proton(s).[13,11] It was found that on irradiation of H-44, the enhancement of H-24 grew at least as quickly as that of H-22. Similarly, on irradiation of H-45, the enhancement of H-22 grew at least as quickly as that of H-24. Thus, the H-22–H-44 distance is approximately equal to the H-24–H-44 distance, and the H-22–H-45 distance is approximately equal to the H-24–H-45 distance. The most plausible structural explanation of this is shown in structure **10**. This structure also includes in-

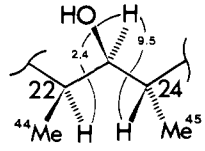

10

formation deduced from the coupling constants between H-22 and H-23 (J = 2.5 Hz) and H-23 and H-24 (J = 9.5 Hz), which suggest that the former pair are gauche and the latter pair are trans. It should be noted that the mirror image of **10** is just as plausible at this stage: thus either **10** or its mirror image could be connected to C-21.

The time courses of the nOes to neighboring protons on irradiation of H-20a, H-20b, H-22, and H-23 were then studied to obtain qualitative information on relative interproton distances. "Direct" nOes, i.e., those that have not arisen via "spin diffusion",[26,27] should buildup exponentially with characteristic $t_{1/2}$'s (the time taken for the enhancements to reach half their maximal values) which are related to r^{-6}, where the values r are the various interproton distances.[13,26,27] The $t_{1/2}$ values for such direct nOes between H-20a, H-20b, H-22, and H-23 and their neighbors are presented in Table V. Comparison of $t_{1/2}$'s between rows of Table V is, perhaps, of questionable validity (the irradiation may not have occurred exactly in the center of each multiplet, there may have been variations in probe temperature between each experiment, etc.) and, in addition, the data are subject to rather large errors. However, within a row (that is, for a single experiment), the $t_{1/2}$ values give a good indication of the rates of buildup of enhancements to the neighboring protons and thus of the relative distances of these neighbors from the irradiated proton. H-22, for example, is seen to be close in space to H-20a, H-20b, and H-23, with H-24 much further away: its closest neighbor is probably H-20a. H-23 is close to H-20a and H-20b, with H-22 more distant: its closest neighbor is probably H-20b. Note that H-23 does not give a direct nOe to H-24, as would indeed be expected from the trans orientation of these two protons shown in **10**.

The coupling constant between H-21 and H-22 is 7.5 Hz; this value is consistent with an approximately trans, or possibly cis, arrangement of these protons. However, the absence of a direct nOe to H-21 upon irradiation of H-22 mitigates against free rotation and against a high population in which H-21 and H-22 are cis, but relatively free rotation about the C-21/C-22 bond cannot be precluded. Using this constraint, and the constraint deduced from the $t_{1/2}$ data that both H-22 and H-23 must be close to *both* H-20a and b, it is concluded that **10** and not its mirror image must represent the configurations at C-22, C-23, and C-24, relative to the arbitrarily defined configuration at C-21. The deduced stereochemistry of this region of pulvomycin, with H-22 trans to H-21, is shown in structure **11**. The configurations at

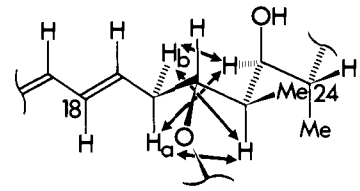

11

C-22, C-23, and C-24, relative to the defined *R* configuration at C-21 are thus *S*, *R*, and *R*, respectively.

The stereochemistries of six of the eight chiral centers in the aglycone have therefore been interrelated, and they are shown in structure **12**. The remaining two, at C-32 and C-33, appear

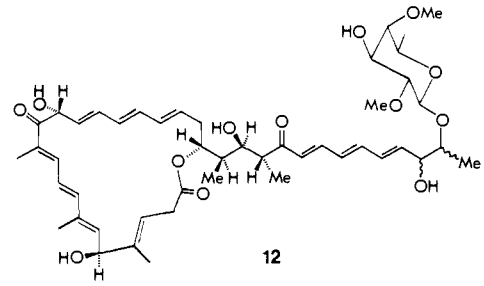

12

not to be accessible by NMR studies on the intact antibiotic. The absolute configurations at these centers and at least one of the interrelated centers are being studied at present by chemical means.

Discussion

In the original structure determination of "labilomycin",[3] the structure of the unusual sugar labilose was demonstrated by comparison of methyl 3-*O*-methyl-α-labiloside, obtained by total methylation (methyl iodide, silver oxide) of methyl α-labiloside, with methyl 6-deoxy-2,3,4-tri-*O*-methyl-α-D-galactopyranoside which was synthesized from β-D-fucose in two steps. The stereochemistry ascribed to labilose is confirmed by the present work. The labilose ^{13}C NMR chemical shifts presented in Table III agree well with the shifts noted by Lukacs et al.[28] for methyl β-labiloside in $(CD_3)_2SO$ solution.

Hydrogenation of labilomycin followed by alkaline and then acid hydrolyses was found by Umezawa et al.[3] to produce a fragment from the antibiotic shown by further degradation work to be 2,3-dihydroxydodeca-10-one. The side chain in structure **2** (C-24 to C-34) can be identified as the precursor to this fragment: hydrogenation of **2** followed by a retro-aldol reaction in base and the cleaving of the glycosidic bond in acid would be expected to give (in a complex mixture of other fragments) this dihydroxy ketone. The carbons of the unusual 22-membered macrocycle presumably escaped detection in the original structure determination because of degradation during (or before) the hydrogenation, which gave rise to small fragments. It can be noted here that, in our hands, hydrogenation under the conditions of Umezawa et al.[3] has failed to give fully hydrogenated pulvomycin,

(26) Bothner-By, A. A.; Noggle, J. H. *J. Am. Chem. Soc.* **1979**, *101*, 5152–5155.
(27) Williamson, M. P.; Williams, D. H. *J. Am. Chem. Soc.* **1981**, *103*, 6580–6585.
(28) Valente, L.; Barata, L. E. S.; Olesker, A.; Rabanal, R.; Lukacs, G.; Thang, T. T. *Tetrahedron Lett.* **1979**, 1149–1152.

as judged by FABMS of the crude hydrogenated product and of the partially separated products. Instead, hydrogenolysis fragments are observed with masses between 250 and 400.

The consequences of this more complex structure for present models of the mode of action[5,29-31] of pulvomycin are unclear. Previously, the perceived structural homology[5] between pulvomycin and kirromycin (**13**) had lead to comparisons which now seem

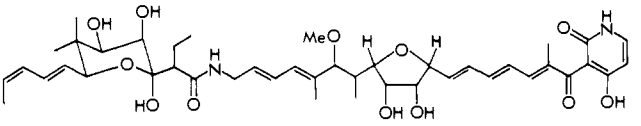

13

tenuous. The "two-site" model for the binding of kirromycin and pulvomycin to EF-Tu (proposed by Pingoud et al.[29]), in which pulvomycin can displace kirromycin from the latter's binding site but the converse cannot occur, cannot now be rationalized on the basis of relative molecular size.

Similarly, the binding constants for the EF-Tu·pulvomycin complex will need to be revised. This may be particularly difficult since spectroscopic measurement does not clearly distinguish between bioactive and bioinactive material (Figure 1).

Preliminary evidence suggests that the lactone ring of pulvomycin may be important for binding to Tu. Mild hydrolysis leads to loss of the characteristic chromophore absorbing at 265 and 275 nm and concomitant loss of bioactivity. Further studies to determine the importance of the macrocycle and its presumably rather unusual biosynthetic origin are presently under way.

Experimental Section

Materials. *N,O*-Bis(trimethylsilyl)-*N*-trifluoroacetamide (Regisil) and *D*-18-*N,O*-bis(trimethylsilyl)-*N*-trifluoroacetamide (Deutro-Regisil) were from Regis Chemical Co., Morton Grove, IL. L-[U-^{14}C]-Phe was from Amersham, France; *E. coli* MRE 600 tRNA^{phe}, poly-U and pyruvate kinase were from Boehringer, Mannheim. MRE 600 frozen cell paste was from CAMR Porton Down, England. Guanosine 5′-triphosphate and phosphoenol pyruvate were from Sigma.

Isolation and Purification of Pulvomycin. Pulvomycin was isolated from *Streptoverticillium netropsis*, MA-2465 obtained as a gift from Dr. Max Tishler, Wesleyan University, Middletown, CT, and Dr. Edward O. Stapley, Merck Institute, Rathway, NJ. A 400-L fermentation of MA-2465 grown as described[4] yielded 18 kg of crude mycelium. This was stable when stored at −70 °C, frozen in 500-g batches. Five hundred grams of crude mycelium was stirred, protected from light, at 4 °C in CH_2Cl_2/MeOH (3:1, v/v; 800 mL) for 48 h. After filtration, the solvent was removed in vacuo, in the dark, and the crude extract stored at −20 °C. The solid mycelium was reextracted with CH_2Cl_2/MeOH in the same manner. Extracts 1 and 2 contained 60% and 30% of the total bioactive material, respectively. Combined crude extracts were dissolved in a small volume of MeOH/EtOAc (3:97, v/v), and pulvomycin was separated by flash chromatography on Kieselgel 60 (0.063–0.20 mm), Merck, elution being carried out with MeOH/EtOAc (3:97, v/v).

Fractions pooled on the basis of TLC and UV analysis were evaporated in the dark under reduced pressure and then subjected to analysis by reverse-phase HPLC. A modular Water Assos. HPLC system was used, consisting of two 6000-A pumps, manual injector U6K, and an automated elution gradient. A Beckman Ultrasphere IP.C-18 column with a CH_3CN–H_2O solvent system (gradient from 30% to 70% CH_3CN (v/v)) was used. UV detection was at 320 or 275 nm on an LC-85 detector from Perkin-Elmer. Pulvomycin, the main peak, had a retention time of 13.7 min and was 92–94% pure based on either absorption at 320 or 275 nm. Such preparations were used for many experiments, but for spectroscopic analysis, pulvomycin was further purified on a Whatman Magnum 9 Partisil 10 ODS-2 column (50 × 1 cm). An isocratic elution nominally using MeOH–H_2O (80/20 v/v) was carried out but the retention time of pulvomycin, and the separation achieved was found to be sensitively dependent on the composition of the eluant. Thus, slight variations of solvent composition were made to achieve optimum results and to ensure that pulvomycin was retained on the column for approximately 20 min. Pulvomycin was collected, and the solvent was removed by evaporation in the dark and stored (20–40 mg/mL in MeOH) under nitrogen at −20 °C. When stored in this manner, pulvomycin is stable for several months, but some decomposition has been found after 6 months.

Bioassay. An overnight culture of *B. subtilis* in N-Broth (0.4 mL) was mixed with top Agar (prepared as described by Miller[32]) (10 mL) and poured on to minimal Agar plates. Pulvomycin, in varying amounts based on λ_{max} 320 nm, $E^{1\%}_{1cm}$ 890, dissolved in MeOH, was applied to filter disks in the usual way. Circles of inhibition were measured after overnight incubation at 37 °C.

In Vitro Protein Synthesis. Elongation factors Tu, Ts, and *G* were purified from MRE 600 solid paste by using the DEAE chromatography procedure of Arai et al.[33] Elongation factor Tu was assayed by a specific filter binding assay by using ^{3}H-GDP at 37 °C.[34] Elongation factor Ts was assayed by its ability to stimulate the Tu ^{3}H-GDP binding assay at 0 °C. Elongation factor *G* was assayed based on its role in poly(U) programmed poly(phenylalanine) synthesis in vitro (essentially as described by Leder[35]). Other components for the assay were purified by standard procedures. Inhibition of poly(phenylalanine) synthesis by pulvomycin was carried out essentially as described by Wittinghofer et al.,[36] in a reaction mixture containing a maximum of 2% MeOH.

Mass Spectrometry. CI (reagent gas CH_4 or NH_3) and EI (electron energy 70 eV) mass spectra were obtained on a Ribermag 10-10C mass spectrometer. Samples were introduced via a direct insertion port, employing either a heated direct insertion probe or a desorption probe with a tungsten filament. FAB mass spectra were obtained on a Kratos MS-50 instrument fitted with an Ion Tech fast atom gun and a high field magnet. Xenon was used as the bombarding species. Samples were transferred to the copper probe tip dissolved in MeOH: the solvent was allowed to evaporate and thiodiglycol (2,2′-thiobis(ethanol)) used as the matrix to dissolve the samples.

Nuclear Magnetic Resonance Spectroscopy. High-resolution ^{1}H and ^{13}C NMR spectra were obtained on a Bruker WH 400 spectrometer at 400.13 and 100.61 MHz, respectively. Spectra were normally accumulated at ambient probe temperature in 8K data points with a spectral width of 10 ppm (^{1}H) or 220 ppm (^{13}C). Proton chemical shifts were either measured downfield from TMS as the internal standard (in CD_3OD) or related to the TMS scale by the relation δ(TMS) = δ-[$(CD_3)_2SO$] + 2.50 (in $(CD_3)_2SO$). The ^{1}H 90° pulse width was 6.5 μs; that of ^{13}C was 12.5 μs. Decoupling difference experiments were performed by using a 25-dB attenuation of the 0.2-W power level, each peak in the spectrum being irradiated in turn using the sequence [blank$_1$ irradiation − (experimental irradiation)$_m$ − blank$_2$ irradiation]$_n$ with m = 18, n = 8 or 16, and with eight transients being recorded for each irradiation frequency before moving to the next frequency. "Blank" spectra were subtracted from experimental spectra on a dedicated Aspect 2000 computer attached to the spectrometer. These decoupling experiments were performed on 10–20 mg of pulvomycin, dissolved in 0.5 mL of the appropriate solvent, as were all other ^{1}H NMR experiments.

The nOe difference experiments were performed by using the irradiation time and power levels given in the footnote to Table III and using the same irradiation sequence given above for the decoupling difference experiments. Studies of the rates of buildup of nOes used the same decoupler power as the nOe difference experiments: the irradiation time, τ_1, was set at 0.2, 0.4, 0.8, 1.6, 3.2, and 6.4 s. Generally one blank frequency was irradiated per two experimental frequencies, for each irradiation time. A minimum of 192 transients was recorded for each irradiation time and frequency, and there was an 8-s delay between the end of one acquisition and the start of the next τ_1. The nOes had generally reached their maximum values after an irradiation time of 3.2 s. The time, $t_{1/2}$, taken to reach half the maximum nOe value was measured from the graph of h_t vs. t, where h_t is the height of the peak in the difference spectrum for an irradiation time t.

The two-dimensional proton–carbon chemical shift correlation experiment was performed on the same Bruker WH-400 instrument as all other NMR experiments, operating at the same ^{1}H and ^{13}C frequencies. A standard Bruker microprogram (Bruker software 1982) was used with quadrature detection in both dimensions and pulse widths of 12.5 μs ($\pi/2$) for carbon and 19.4 μs ($\pi/2$) for proton via the decoupler coils. The delay τ_1 was set at 0.0033 s to allow optimum polarization transfer for a J_{CH} value of 150 Hz. The refocusing time $\tau 2$ was set at 0.00165

(29) Pingoud, A.; Block, W.; Urbanke, C.; Wolf, H. *Eur. J. Biochem.* **1982**, *123*, 261–265.
(30) Pingoud, A.; Block, W.; Wittinghofer, A.; Wolf, H.; Fischer, E. *J. Biol. Chem.* **1982**, *257*, 11 261–11 267.
(31) Wolf, H.; Fischer, E. *Antibiotics (N.Y.)* **1983**, *6*, 71–89.
(32) Miller, J. H. "Experiments in Molecular Genetics"; Cold Spring Harbor Lab.; Cold Spring Harbor, NY, 1972.
(33) Arai, K.-I.; Kawakita, M.; Kaziro, Y. *J. Biol. Chem.* **1972**, *247*, 7029–7037.
(34) Furano, A. V. *Proc. Natl. Acad. Sci. U.S.A.* **1975**, *72*, 4780–4784.
(35) Leder, P. *Methods Enzymol.* **1971**, *20*, 302–306.
(36) Wittinghofer, A.; Frank, R.; Gast, W. H.; Leberman, R. *J. Mol. Biol.* **1979**, *132*, 253–256.

s, and a recycle time of 0.9 s was used. The spectral widths selected were 16129 Hz (160 ppm) for carbon and ±1410 Hz for proton, with an initial data matrix size of 256 W × 4K (t_1, t_2). The data were processed in the usual fashion. The experiment was performed on approximately 50 mg of pulvomycin, dissolved in 0.5 mL of CD_3OD, and accumulation of data required approximately 14 h.

Acknowledgment. We thank Dr. Tishler (Wesleyan University) and Dr. Stapley (Merck Institute) for making the strain MA-2465 available to us and Mlle Gerardot and Dr. Monteil (Institut de Bacteriologie, Strasbourg) for the strain of *B. subtilis*. We also thank the Science and Engineering Research Council for financial support.

Registry No. 12, 95740-54-8.

The Generation and Trapping of the High-Temperature Cation Radicals $^{28}SiO^+$ and $^{29}SiO^+$ in Neon Matrices at 4 K; An ESR and ab Initio CI Theoretical Investigation

Lon B. Knight, Jr.,*† A. Ligon,† R. W. Woodward,† David Feller,‡ and E. R. Davidson‡

Contribution from the Chemistry Departments, Furman University, Greenville, South Carolina 29613, and the University of Washington, Seattle, Washington 98195.
Received September 17, 1984

Abstract: The high-temperature cation radicals $^{28}SiO^+$ and $^{29}SiO^+$ have been generated by both electron bombardment and photoionization methods and trapped in neon matrices at approximately 4 K for detailed ESR (electron spin resonance) studies. The SiO(g) sample was prepared by the high-temperature (≈2000 K) vaporization of SiO(s) and SiO_2(s). The magnetic parameters obtained for $^{29}SiO^+$ in neon are the following: $g_\parallel = 2.0012$ (2); $g_\perp = 2.0000$ (2). For ^{29}Si $A_\parallel = -924$ (1) MHz and $A_\perp = -733$ (1) MHz. Analysis of the SiO^+(g) tensor clarifies the assignment of an electronic band ($X^2\Sigma \leftarrow B^2\Sigma$) previously associated with both SiO^+ and SiN. Extensive ab initio calculations have been conducted which yield ^{29}Si hfs in good agreement with the experimental results, although redefinition of orbitals used in the CI via MCSCF or INO procedures was required. A population analysis of the valence orbitals for SiO^+, CO^+, AlO, and BO has been made with the results compared to those obtained from the commonly applied procedure for estimating percent "s" or "p" character from "free atom" hyperfine parameters. Significant differences between the two methods were obtained for SiO^+ and AlO. A major deficiency of the free atom comparison method in these two cases was attributed to oxygen valence overlap effects on the core electrons of the metal.

The ESR (electron spin resonance) rare gas matrix isolation technique has been used to investigate several high-temperature (>1000 K) neutral radicals;[1-4] however, no high-temperature cation (or anion) radicals have been studied. Gas-phase ESR measurements of such radicals cannot be conducted by currently available methods. These results for SiO^+ demonstrate the feasibility of combining high-temperature vaporization with the various ion generation and neon matrix trapping techniques developed in recent studies of $^{13}CO^+$,[5,6] $^{15}N_2^+$,[7] $H_2{}^{17}O^+$,[8] $H_2{}^{13}CO^+$,[9] CH_4^+,[10] and Cd^+.[11] Application of the methods to numerous other important inorganic and nonvolatile systems should be straightforward. These techniques have already been adapted for the matrix trapping of ion–neutral reaction products such as $C_2O_2^+$[12] and N_2CO^+[13] and the paramagnetic metal cluster cations Mg_2^+, Mg_3^+, and Mg_6^+.[13] Laser vaporization/ionization methods for trapping cation radicals of refractory materials and matrix codeposition reactions of metal ions with various volatile reagents are currently being investigated by matrix ESR in our laboratory.

The $SiO^+(X^2\Sigma)$ species was selected to be the first high-temperature candidate investigated in detail for the following reasons. Magnetic data comparison with $CO^+(X^2\Sigma)$ can be used to probe electronic and bonding changes that occur as carbon is replaced by silicon in a "simple" diatomic molecule. Detailed comparison of ^{29}Si ($I = {}^1/_2$) nuclear hfs (hyperfine structure) in $^{29}SiO^+$ with previously reported ^{13}C hfs of $^{13}CO^+$ is presented. Experimental conditions for the high-temperature formation of SiO(g) have been established in earlier vibrational (IR) matrix experiments[14,15] which were repeated at the beginning of this study to ascertain that neutral SiO(g) was being generated in reasonable quantities prior to the application of ionization techniques. Magnetic parameters for SiO^+ are particularly interesting since it is isoelectronic to the previously studied high-temperature neutral radical AlO.[16] Electronic structures of these radicals are compared by both theoretical and experimental results. Distinguishing between the electronic bands of SiO^+ and SiN has proven to be a difficult problem.[17,18,19] The **g** tensor measurements obtained in this study

† Furman University.
‡ University of Washington.

(1) Weltner, W., Jr. "Magnetic Atoms and Molecules"; Van Nostrand-Reinhold Co., Inc.: New York, 1983.
(2) Kasai, P. H.; Whipple, E. B.; Weltner, W., Jr. *J. Chem. Phys.* **1966**, *44*, 2581.
(3) Knight, L. B., Jr.; Wise, M. B.; Fisher, T. A.; Steadman, J. *J. Chem. Phys.* **1981**, *74*, 6636.
(4) Lindsay, D. M.; Thompson, G. A. *J. Chem. Phys.* **1982**, *77*, 1114. Howard, J. A.; Sutcliffe, R.; Tse, J. S.; Mile, B. *Chem. Phys. Lett.* **1983**, *94*, 561. Baumann, C. A.; Van Zee, R. L.; Bhat, S. V.; Weltner, W., Jr. *J. Chem. Phys.* **1983**, *78*, 190.
(5) Knight, L. B., Jr.; Steadman, J. *J. Chem. Phys.* **1982**, *77*, 1750–1756.
(6) Knight, L. B., Jr.; Steadman, J. *J. Am. Chem. Soc.* **1984**, *106*, 900–902.
(7) Knight, L. B., Jr.; Bostick, J. M.; Woodward, R. W.; Steadman, J. *J. Chem. Phys.* **1983**, *78*, 6415.
(8) Knight, L. B., Jr.; Steadman, J. *J. Chem. Phys.* **1983**, *78*, 5940.
(9) Knight, L. B., Jr.; Steadman, J. *J. Chem. Phys.* **1984**, *80*, 1018–1025.
(10) Knight, L. B., Jr.; Steadman, J.; Feller, D.; Davidson, E. R. *J. Am. Chem. Soc.* **1984**, *106*, 3700.
(11) Knight, L. B., Jr.; Miller, P. K.; Steadman, J. *J. Chem. Phys.* **1984**, *80*, 4587.
(12) Knight, L. B., Jr.; Steadman, J.; Miller, P. K.; Bowman, D. E.; Davidson, E. R.; Feller, D. *J. Chem. Phys.* **1984**, *80*, 4593.
(13) Knight, L. B., Jr.; Steadman, J.; Ligon, A.; Barnett, C. D., to be published.
(14) Anderson, J. S.; Ogden, J. S. *J. Chem. Phys.* **1969**, *51*, 4189.
(15) Hastie, J. W.; Hauge, R. H.; Margrave, J. L. *Inorg. Chim. Acta* **1969**, *3*, 601.
(16) Knight, L. B., Jr.; Weltner, W., Jr. *J. Chem. Phys.* **1971**, *55*, 5066.

0002-7863/85/1507-2857$01.50/0